PRELIMINARY VALIDATION OF SERPENT2/SUBCHANFLOW USING THE SPERT IV D-12/25 DATA

J.C. ALMACHI, V.H. SANCHEZ-ESPINOZA
Institute for Neutron Physics and Reactor Technology, Karlsruhe Institute of Technology
Hermann-von-Helmholtz-Platz 1, 76344 Eggenstein-Leopoldshafen – Germany

ABSTRACT

This paper describes the preliminary validation of Serpent2/Subchanflow using data from SPERT IV reactor loaded with plate-type fuel. The transient test selected for this analysis was B-35, which is a part of the SPERT IV D-12/25 test program. This test involves the insertion of reactivity by single and combined movements of the transient rod. A total of 5 cases are proposed, where in the first four cases the transient rod reaches a constant withdrawal velocity of -33, -32, -30, and -27 cm/s within a time interval of 0.16 s. In the fifth case, a combined withdrawal and insertion of the transient rod was performed with velocities of -32 cm/s and 3 cm/s in time intervals of 0.16 s and 0.12 s. The maximum reactivity obtained with this set of tests was 1.03 $\pm$ 0.04 \$, which corresponds to Case-1. The predictions performed for Case-5 with a reactivity of 0.98 $\pm$ 0.04 \$ added to the core were in better agreement with the experimental data than those for the other cases.

1. Introduction

Numerical codes have become key tools in the simulation and analysis of nuclear power and research reactors. The types of programs used include neutronic and thermal-hydraulic codes, which are selected according to the level of detail of the application and the computational resources. Monte Carlo codes such as Serpent 2 are used for neutron analysis and allow for steady-state, transient, and burnup calculations [1,2]. The geometric configurations that can be handled by Serpent 2 are broad, so it can be used for neutron analysis of power and research reactors [3]. On the other hand, there are thermal-hydraulic codes that can be used to model the behavior of the coolant and heat transfer in the reactor. In general, thermal-hydraulic system codes are mostly developed for applications of power reactors. Thus, if research reactors are to be analyzed using these codes, some heuristic assumptions and modifications must be made [4]. When codes are extended or modified, it is mandatory that they go through the verification and validation phases [5,6]. For the validation phase, experimental data of appropriate tests are used for comparison with the code predictions. The experimental data obtained in the reactor SPERT IV is unique and very valuable to validate numerical codes. In [7–9] recommendations can be found about how to proceed to properly model the SPERT IV reactor for validation purposes. In this work, the capability of high-fidelity code Serpent2/Subchanflow to model steady-state and transient conditions of plate-type fuel assemblies loaded in the SPERT IV reactor is validated for the first time.

This paper consists of six chapters, where the first two briefly discuss the main features of Serpent 2 and Subchanflow. Chapter 3 describes the core configuration of the SPERT IV reactor and the initial parameters immediately prior to the transient test. Chapter 4 explains the key assumptions and simplifications used to model SPERT IV core with Serpent 2 and Subchanflow. Chapter 5 discusses the predictions of the core behavior in case of a reactivity insertion and compares measurements with the predicted values. Finally, Chapter 6 provides a summary and outlook of this research.

2. Calculations tools

The neutronic Monte Carlo code Serpent v2.1.32 and the thermal-hydraulic code Subchanflow v.3.7.1 were used for the analysis of the reactivity insertion experiment at the reactor SPERT IV D-12/25 test. Both codes were coupled using the master-slave approach developed at the Karlsruhe Institute of Technology [10].

2.1 Serpent 2

Serpent 2 allows the simulation of steady-state, transient, and burnup problems [2]. It is a widely used due to its detailed geometrical representation of the cores almost without simplifications of complicated geometry. Hence it is ideal for modeling power reactors and research reactors. It uses the continuous energy standard ACE format cross-section libraries for neutron and photon transport physics. Among different nuclear data libraries, the following formats can be used in Serpent 2: ENDF/B-VIII.0, JEFF-3.2, JENDL-4.0, etc. Serpent 2 also includes the very flexible multiphysics interface for coupling with different solvers (thermal-hydraulics, thermal-mechanics) to handle the exchange of feedback parameters such as density and fuel temperature, boron concentration, etc. For multiphysics applications, the rejection sampling techniques are used in combination with target motion sampling to consider the scattering of neutrons in a moderator medium [1, 11].

2.2 Subchanflow

Subchanflow is a thermal-hydraulic subchannel code developed at the Karlsruhe Institute of Technology for the analysis of power reactors such as LWRs or VVERs [12]. The latest validated and released update allows the modeling of research reactors with plate-type fuel [4, 5, 13]. Subchanflow is a very flexible code allowing a channel-wise and a subchannel-wise simulation as stand-alone or coupled with different neutronic solvers e.g. nodal diffusion (PARCS, DYN3D), low-order transport (DYN3D-SP3, PARCS), Monte Carlo (Serpent 2, MCNP), and thermal-mechanic (TRANSURANUS) solvers [6, 14, 15].

2.3 Serpent2/Subchanflow coupling approach

Serpent 2 and Subchanflow are coupled based on the master-slave approach, where Serpent 2 acts as the master and Subchanflow as the slave. In this approach, local feedback parameters are exchanged between the different solvers. Figure 1 (a) shows the parameter exchange, where the Monte Carlo code calculates the power generated by nuclear fission and transfers it to the thermal-hydraulic code. The thermal-hydraulic code calculates the temperature and density parameters of fuel and coolant and exchanges its results with the Monte Carlo code until a certain convergence is reached. The exchange of thermal-hydraulic fields is handled internally using overlay files called IFCs. For complicated geometries, the option of remapping axial and radial nodes is also enabled [1, 11, 16].

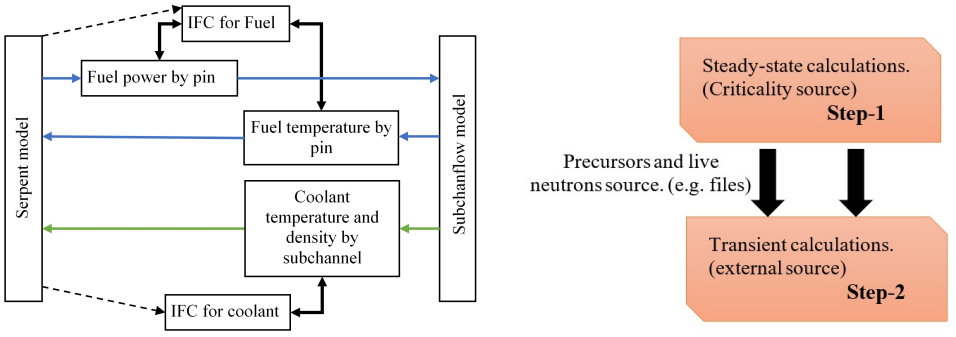

(a) (b)

Fig. 1. Concepts used for: (a) thermal-hydraulic field exchange in coupled system; (b) two-step scheme for transient simulations.

For dynamic simulations, Serpent 2 uses the two-step transient approach (see Figure 1 (b)). In the first phase, a static criticality source simulation is done to compute $K_{eff} = 1$. This simulation is needed to predict the source of live neutrons and the source of neutron precursors that are used in the second step as external neutron sources. The live neutrons travel with a given position, direction and energy, and the precursor population is the one that generates the delayed neutrons. In the second phase, an external source transient calculation is performed using the previously calculated external sources. This approach allows for changes in the surfaces where neutrons interact, so it is helpful for modeling transient scenarios, e.g., control rod ejection transients [1, 11, 16].

3. Brief description of the SPERT IV facility

Figure 2 shows the Special Power Excursion Reactor (SPERT) built under the U.S. Atomic Energy Commission's reactor safety program. Neutronic and thermal-hydraulic tests were conducted in July 1962 at SPERT IV D-12/25. The tests were performed at steady-state and transient conditions and the results are documented in [8, 17]. The core was loaded with 20 standard fuel assemblies of plate-type fuel, and 5 control fuel assemblies forming a 5x5 square core. Each standard fuel assembly is composed of 12 thin plates spaced 4,547 mm apart. The control fuel assemblies contain a total of 6 plates, 4 of which are placed in the center and one at each end, the excess space formed by the absence of the remaining 6 plates is occupied by the control rods and the transient rod.

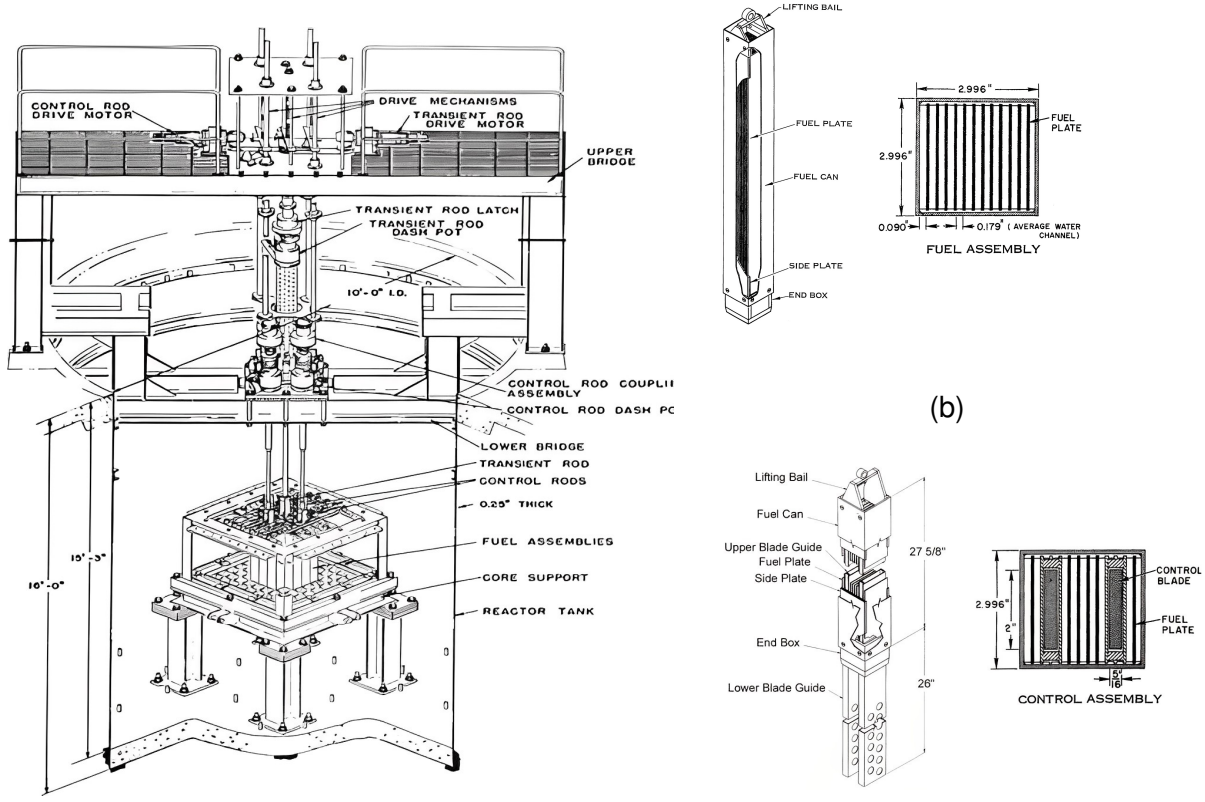

Fig. 2. SPERT experimental reactor facilities obtained from [7]: (a) representation of the reactor; (b) standard fuel assembly; (c) control/transient fuel assembly.

Figure 3 shows the reactor core and the position of each fuel assembly within an aluminum matrix. The transient rod is located in the center and the control rods are symmetrically arranged around the core. The main difference between the transient rods and the control rods is the location of the poisonous material (B-Al), which is located in the lower region for the transient rod and in the upper region for the control rods. A detailed geometrical description of the elements that make up the SPERT reactor in international units can be found in [3].

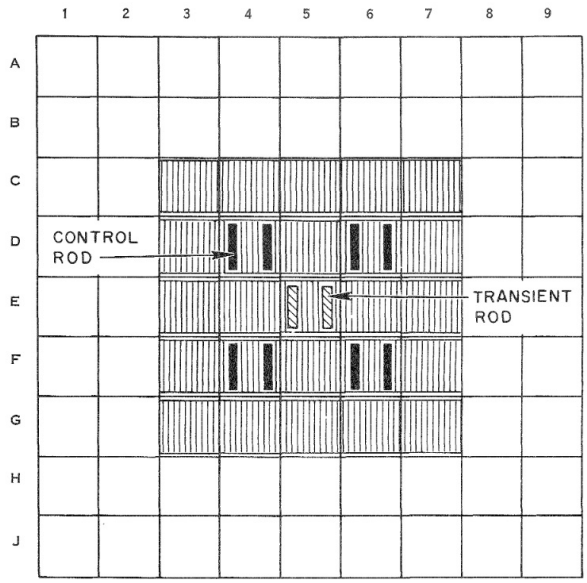

Fig. 3. Schematic representation of the SPERT IV D-12/25 core loading obtained from [7].

Table 1 shows the main operating specifications for the test SPERT IV D-12/25 B-35 before the transient event. Additional information on the atomic density of materials for Monte Carlo calculations can be found on [7] page 14.

Type of reactor	**Open pool MTR type**
Fuel type	UAl alloy Al clad flat plate fuel
Enrichment	HEU 93 %, 14.0 g ^{235}U
Reference pressure	Pool is open to the atmosphere
Nominal reference temperature	22 °C
Coolant, moderator, reflector	Light water
Poison material	Binal (B-Al)
Initial power	68495.18 [W]
Coolant flow rate	3.87 [m/s]
External reactivity	1.05 $

Tab 1: Initial steady-state prior the transient event.

4. Development of the SPERT-IV models

4.1 Serpent 2 model

Since this is the first time that the SPERT IV D-12/25 B-35 tests are going to be analyzed with high-fidelity tools like Serpent2/Subchanflow, some assumptions are needed for the creation of the three-dimensional model of Serpent 2 such as:

- The composition of the main materials was obtained from [7] and will be addressed using the nuclear data library ENDFB-VIII.0.
- For the initial criticality calculation, 200 inactive cycles with 1000 active cycles composed of 1E6 histories are used.
- Each fuel plate is divided into 20 axial zones.
- Reactivity addition to the core is performed by the transient rod (TR), for which the critical state calculated in [3] is used; Figure 4 shows the position of the control bars and the transient bar.
- For the transient simulations, a total particle number of 4E6 with a number of batches of 200 is used.
- For the transient simulation with Serpent2/Subchanflow, a time interval of 4 s is considered, divided into 100 bins with a step of 0.04 s, so that the initial and final times within Serpent2/Subchanflow will be t_o = 0 s and t_f = 4 s, respectively.
- The experimental power values measured in test B-35 start at t_1 = 0.89 s and end at t_2 = 7.05 s. These times are extensive for the Monte Carlo calculations, so to reduce the calculation time, the time interval is shortened. To determine the new interval, 4 s are added to time t_1, resulting in a final time of 4.89 s. In summary, for test B-35, the initial and final time will be t_o = 0.89 s and t_f = 4.89 s, respectively.

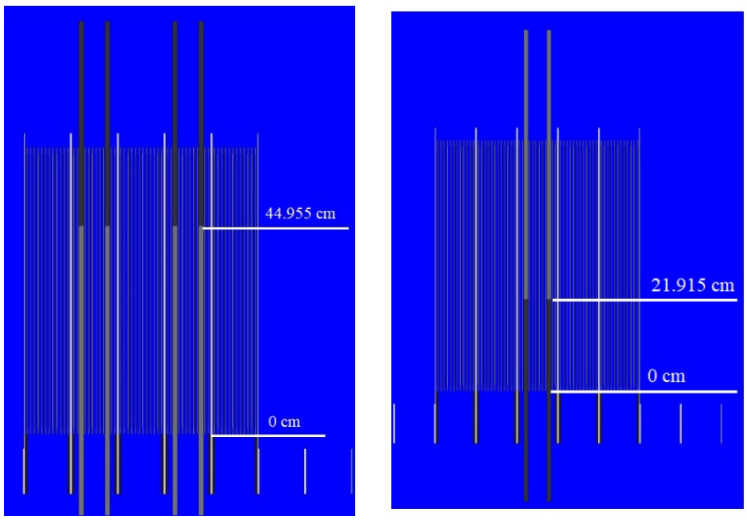

(a) (b)

Fig. 4. Critically state; axial section to identify the position of: (a) control rods; (b) transient rod.

4.2 Subchanflow model

The detailed subchannel-level model of the SPERT-IV core is developed for Subchanflow with the following assumptions:

- Sub-channel centered plate model was considered.
- The radial discretization of the plate is divided into 3 nodes for the fuel and 2 for the cladding.
- The axial discretization for each coolant and plate is 20 nodes.
- The Y-Sudo and Blasius correlations for heat transfer and pressure drop are used.

5. Discussion of preliminary results

5.1 Serpent2/Subchanflow coupling approach

A total of 46 transient tests with reactivity addition were performed and described in [9]. In this work, the B-35 test is analyzed in detail and the data is used for code validation. Currently, there are records of certain tests that are mainly used for code validation. Among the most common tests are the B-34 and B-35 tests, which, according to the literature, have the must significant discrepancy between measured and calculated values, so it is recommended to use more robust methods and extensions of certain correlations to adjust the results [18,19]. Figure 5 shows the experimental evolution of the power until a time of 4.89 seconds is reached. In this figure, a rapid increase in power can be seen from time t = 0.89 s, suggesting a sudden rise in reactivity; subsequently, it can be observed that the trend of the curve starts to change at time t = 1.54 s, until time t = 2.74 s, where the trend of power evolution changes again. The changes in the trend of power evolution may be due to adjustments in reactivity during the test, so in principle the possibility of additional movements should be considered before defining the transient bar movement scenario.

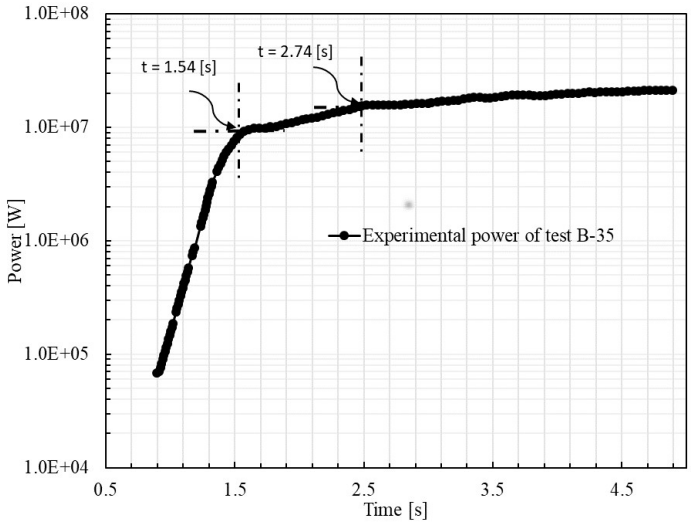

Fig. 5. Experimental power evolution for the B-35 test.

Table 2 shows 4 cases proposed to simulate the speed of withdrawal of the transient rod (TR) of the B-35 test, where different speeds can be observed for the same time interval. The aim is to predict the reactivity curve and see how it affects the power curve.

ID	Vel [cm/s]	Time scope [s]
Case-1	-33	0.89 - 1.05
Case-2	-32	0.89 - 1.05
Case-3	-30	0.89 - 1.05
Case-4	-27	0.89 - 1.05

Tab 2: TR withdrawal velocities models.

5.2 Discussion of the results for B-35 test

Figure 6 shows the Serpent2/Subchanflow predicted reactivity for the 4 cases proposed in Table 2. In all cases, a sudden increase in reactivity is observed in the first few seconds until

a maximum value is reached, then the predicted reactivity values decrease, stabilization of reactivity would be the expected behavior for a long time.

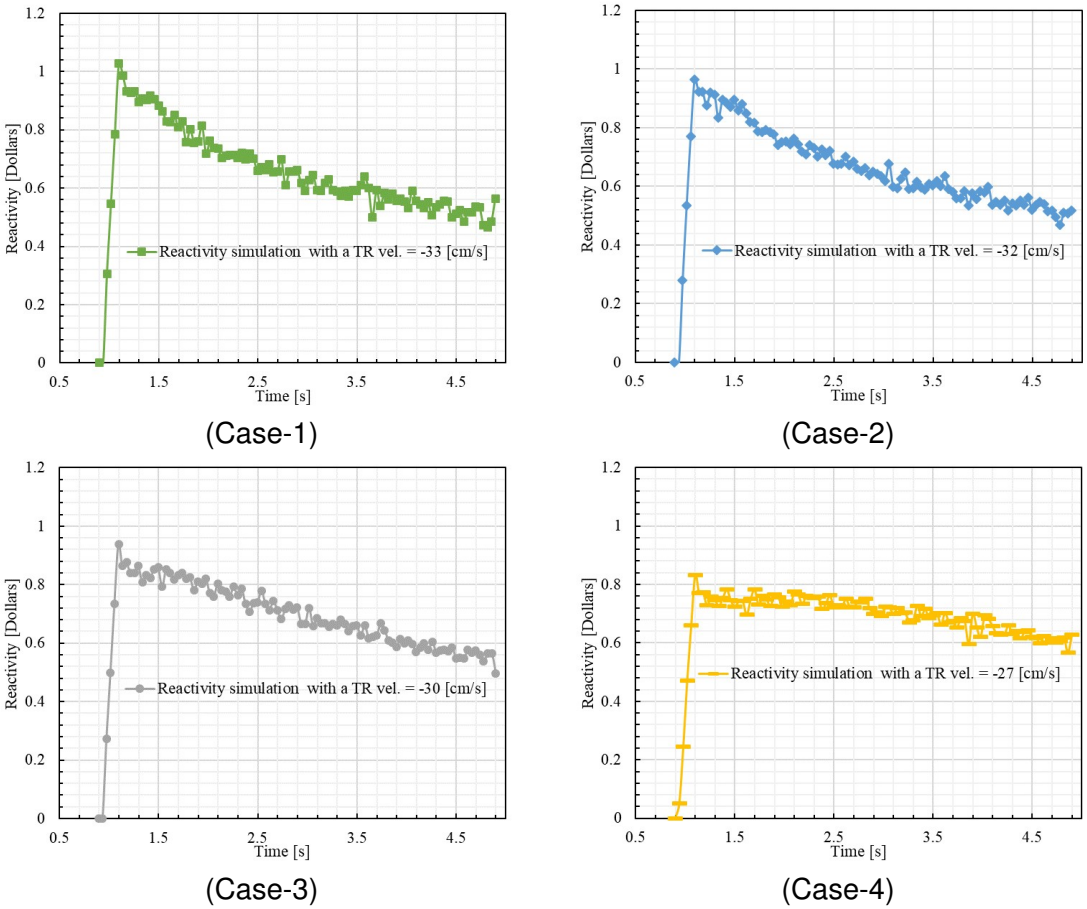

Fig. 6. Reactivity inserted to the core by the withdrawal movement of the TR at various velocities.

Table 3 shows the maximum predicted reactivity values for the cases shown in Table 2. It can be seen that the reactivity values for Case-4 and Case-3 are significantly lower than the reactivity value recorded in test B-35, from which it can be inferred that the predicted power curves for Case-4 and Case-3 will be lower than the experimental values.

ID	SSS2/SCF reactivity [$]	Referent reactivity [$]
Case-1	1.03 ± 0.04	1.05
Case-2	0.97 ± 0.04	1.05
Case-3	0.94 ± 0.04	1.05
Case-4	0.83 ± 0.04	1.05

Tab 3: Maximum reactivity values predicted by Serpent2/Subchanflow.

Figure 7 shows various power evolutions predicted by Serpent2/Subchanflow for the B-35 test. It can be seen that Case-4 and Case-3, which have a withdrawal velocity of -27 and -30 cm/s, are not sufficient to predict the power values at the beginning of the test, so these cases can be discarded. Case-1, whose velocity is -33 cm/s, overestimates the power values in almost the entire period, which could lead to an erroneous estimation of the temperature profiles of the coolant and fuel assembly. On the other hand, Case-2 over-predicts the power values and underestimates them, but shows good agreement with the experimental values at least

before the time 1.54 s. In summary, Case-2 is a candidate for adding transient rod insertion motions to reduce power; the additional intervals shown in Table 4 are performed considering the approximate points in Figure 5.

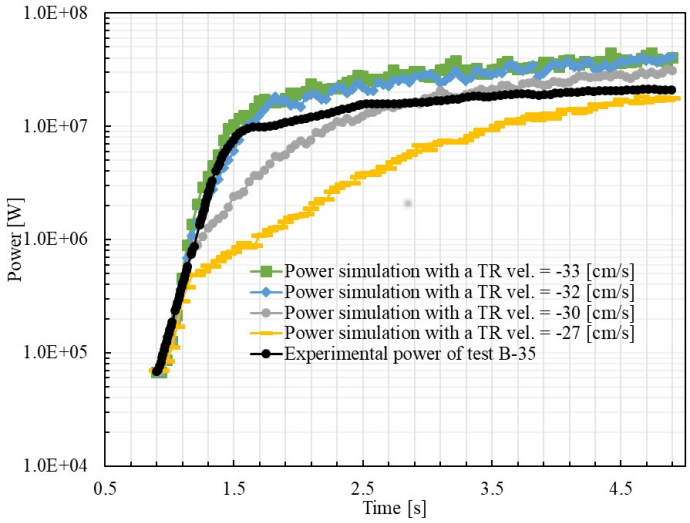

Fig. 7. Power evolution predicted by Serpent2/Subchanflow compared to experimental values.

ID	Vel1 | Time scope	Vel2 |Time scope	Vel3 | Time scope
Case-5	-32 | 0.89 - 1.05	3 | 1.61 - 1.73	3 | 2.73 – 2.85
Vel [cm/s], Time scope [s].			

Tab 4: TR withdrawal/insertion velocities models.

Figure 8 shows the Serpent2/Subchanflow predicted reactivity values for Case-5 and Case-2. It can be seen that Case-5 reaches a maximum reactivity value of 0.98 $\pm$ 0.04 \$, which is slightly higher than that of Case-2 (see Table 3). In Case-5, the movements of withdrawal and insertion of the transient rod were combined, so the reactivity curve has two points that deviate slightly from the continuity of the curve, although no significant differences are observed.

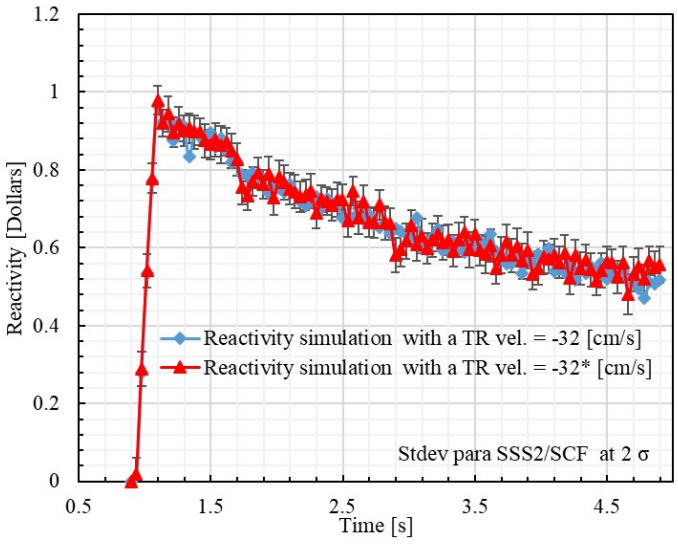

Fig. 8. Reactivity inserted to the core, Case-5 and Case-2.

Finally, Figure 9 compares of the experimental power values with those predicted by Serpent2/Subchanflow. It can be observed that the predicted results show a good agreement with the experimental values. In general, no significant difference is observed between the two curves, and most of the experimental values are within the $\pm$ 2 sigma error bar.

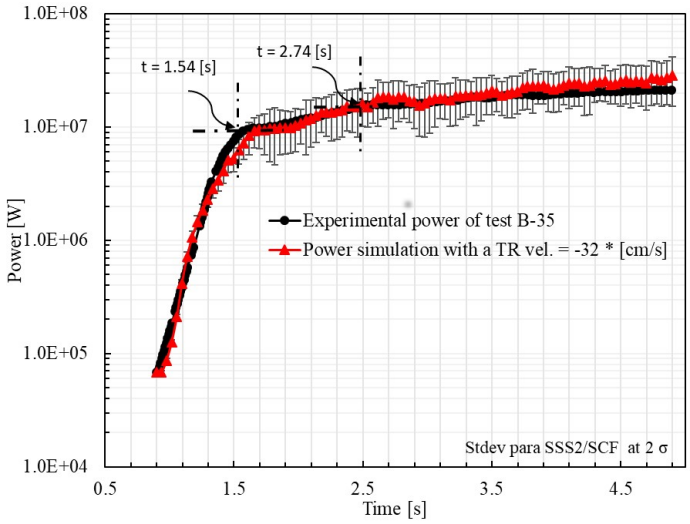

Fig. 9. Power evolution predicted by Serpent2/Subchanflow (Case-5) compared to experimental values.

5.3 Computational resources

All simulated cases in this paper were run on the HoreKa supercomputer at KIT. HoreKa is an innovative hybrid system with nearly 60,000 Intel processor cores, over 250 terabytes of main memory, and 668 NVIDIA A100 GPUs. Hybrid compilation between 2 MPI nodes and 152 OMP cores was used for a total of 304 cores per simulation. The run times for each case are summarized in Table 5.

ID	Running time [hr.mm.ss]	Cores per node
Case-1	58:32:31	152
Case-2	60:14:01	152
Case-3	58:40:11	152
Case-4	58:03:25	152
Case-5	60:29:03	152
Average node power draw: 641.22 watt.		

Tab 5: Running times associated with the coupling scheme.

6. Summary and outlook

A detailed analysis of reactivity insertion in the reactor SPERT IV D-12/25 was performed using the Serpent2/Subchanflow codes. Five reactivity insertion scenarios were used to simulate the B-35 test. The scenario designated as Case-5 showed the best agreement with the experimental results. Reactivity insertion into the reactor core was performed by the combined motion withdrawal and insertion of the transient rod. The maximum reactivity

values determined for Case-5 were 0.98 $\pm$ 0.04 s, about 6.6% lower than the reference value. Approximately 294 hours of computational time on an HPC were used to simulate all cases. The results presented in this paper are the first step towards the validation of the Serpent2/Subchanflow code for MTR research reactors.

Acknowledgments
The authors acknowledge the financial support of the NUSAFE program at the Karlsruhe Institute of Technology (KIT). This work was performed on the HoreKa supercomputer funded by the Ministry of Science, Research and the Arts Baden-Württemberg and by the Federal Ministry of Education and Research.

References

[1] J. Leppänen, "Modeling of Nonuniform Density Distributions in the Serpent 2 Monte Carlo Code," Nuclear Science and Engineering, vol. 174, no. 3, pp. 318-325, 2013. [CrossRef]

[2] J. Leppänen, M. Pusa, T. Viitanen, V. Valtavirta and T. Kaltiaisenaho, "The Serpent Monte Carlo code: Status, development and applications in 2013," Annals of Nuclear Energy, vol. 82, pp. 142-150, 2015. [CrossRef]

[3] J. C. Almachi and V. H. Espinoza-Sanchez, "Validation of Serpent 2 using experimental data from the SPERT-IV D-12/25," In Proceedings of the European Research Reactor Conference, Budapest, Hungary, 6–10 June, ISBN: 978-92-95064-38-6, pp. 142-150, 2021. [CrossRef]

[4] J. C. Almachi, V. Sánchez-Espinoza and U. Imke, "Extension and validation of the SubChanFlow code for the thermo-hydraulic analysis of MTR cores with plate-type fuel assemblies," Nuclear Engineering and Design, vol. 379, 2021. [CrossRef]

[5] J. C. Almachi and V. H. Espinoza-Sanchez, "Extension of the validation basis of Subchanflow by using measured data from the IEA-R1 research reactor," In Proceedings of XXXIII Congreso Anual de la Sociedad Nuclear Mexicana, Energía Nuclear: La fuente de energía más eficiente para mitigar el calentamiento global, Veracruz, Mexico, 13-16 November, pp. 1-13, 2022. [CrossRef]

[6] D. Ferraro, M. García, V. Valtavirta, U. Imke, R. Tuominen, J. Leppänen and V. Sanchez-Espinoza, "Serpent/SUBCHANFLOW pin-by-pin coupled transient calculations for the SPERT-IIIE hot full power tests," Ann. Nucl. Energy, vol. 142, p. 107387, 2020. [CrossRef]

[7] S. Day, "SPERT IV D-12/25: Facility specification," International Atomic Energy Agency (IAEA), Hamilton, Canada, 2015. [CrossRef]

[8] J. G. Crocker, J. E. Koch, Z. R. Martinson, A. M. Mcglinsky and L. A. Stephen, "NUCLEAR START-UP OF THE SPERT IV REACTOR," Technical Report: IDO-16905, NSA-17-040407, Phillips Petroleum Co. Atomic Energy Div., Idaho Falls, Idaho, United States, 1963. [CrossRef]

[9] J. G. Crocker and L. A. Stephan, "REACTOR POWER EXCURSION TESTS IN THE SPERT IV FACILITY," Technical Report: IDO-17000, NSA-18-044970, Phillips Petroleum Co. Atomic Energy Div., Idaho Falls, Idaho, United States, 1964. [CrossRef]

[10] D. Ferraro, M. García, V. Valtavirta, U. Imke, R. Tuominen, J. Leppänen and V. Sanchez-Espinoza, "Serpent/SUBCHANFLOW pin-by-pin coupled transient calculations for a PWR minicore," Ann. Nucl. Energy, vol. 137, p. 107090, 2020. [CrossRef]

[11] V. Valtavirta, "Development and applications of multiphysics capabilities in a continuous energy Monte Carlo neutron transport code (Ph.D. thesis)," Aalto University, School of Science, Department of Applied Physics, Finland, ISBN: 978-952-60-7377-4, 2017, 2017. [CrossRef]

[12] U. Imke and V. Sanchez-Espinoza "Validation of the Subchannel Code SUBCHANFLOW Using the NUPEC PWR Tests (PSBT)," Science and Technology of Nuclear Installations, 2012. [CrossRef]

[13] J. C. Almachi, U. Imke and V. H. Espinoza-Sanchez, "Extensions of Subchanflow for Thermal Hydraulic Analysis of MTR-Cores," In Proceedings of the European Research Reactor Conference, Online, 12–15 October, ISBN: 978-92-95064-34-8, pp. 1-10, 2020. [CrossRef]

[14] M. García, R. Vočka, R. Tuominen, A. Gommlich, J. Leppänen, V. Valtavirta, U. Imke, D. Ferraro, P. Van-Uffelen, L. Milisdörfer and V. Sanchez-Espinoza, "Validation of Serpent-SUBCHANFLOW-TRANSURANUS pin-by-pin burnup calculations using experimental data from the Temelín II VVER-1000 reactor," Nuclear Engineering and Technology, vol. 53, no. 10 p. 3133-3150, 2021. [CrossRef]

[15] J. C. Almachi , V. H. Sánchez-Espinoza and U. Imke, "High-Fidelity Steady-State and Transient Simulations of an MTR Research Reactor Using Serpent2/Subchanflow," Energies, vol. 15, no. 4, p. 1554, 2022. [CrossRef]

[16] D. Ferraro, "Monte Carlo-based multi-physics analysis for transients in Light Water Reactors (Ph.D. thesis)," In the Institute for Neutron Physics and Reactor Technology (INR) of Karlsruhe Institute of Technology (KIT), Germany, KITopen-ID: 1000131803, 2021. [CrossRef]

[17] R. W. Miller, A. Sola and R.K. McCardell "REPORT OF THE SPERT I DESTRUCTIVE TEST PROGRAM ON AN ALUMINUM, PLATE-TYPE, WATER-MODERATED REACTOR," Technical Report: IDO-16883, NSA-18-035220, Phillips Petroleum Co. Atomic Energy Div., Idaho Falls, Idaho, United States, 1964. [CrossRef]

[18] J.-M. Labit, N. Seiler, O. Clamens and E. Merle, "Thermal-hydraulic two-phase modeling of reactivity-initiated transients with CATHARE2 – Application to SPERT-IV simulation," Nuclear Engineering and Design, vol. 381, 2021. [CrossRef]

[19] M. Margulis and E. Gilad, "Simulations of SPERT-IV D12/15 transient experiments using the system code THERMO-T," Progress in Nuclear Energy, vol. 109, pp. 1-11, 2018. [CrossRef]